



The ACT/MaDCoWS Mass/Richness Scaling Relation

Jack Orlowski-Scherer, Grad Student, University of Pennsylvania

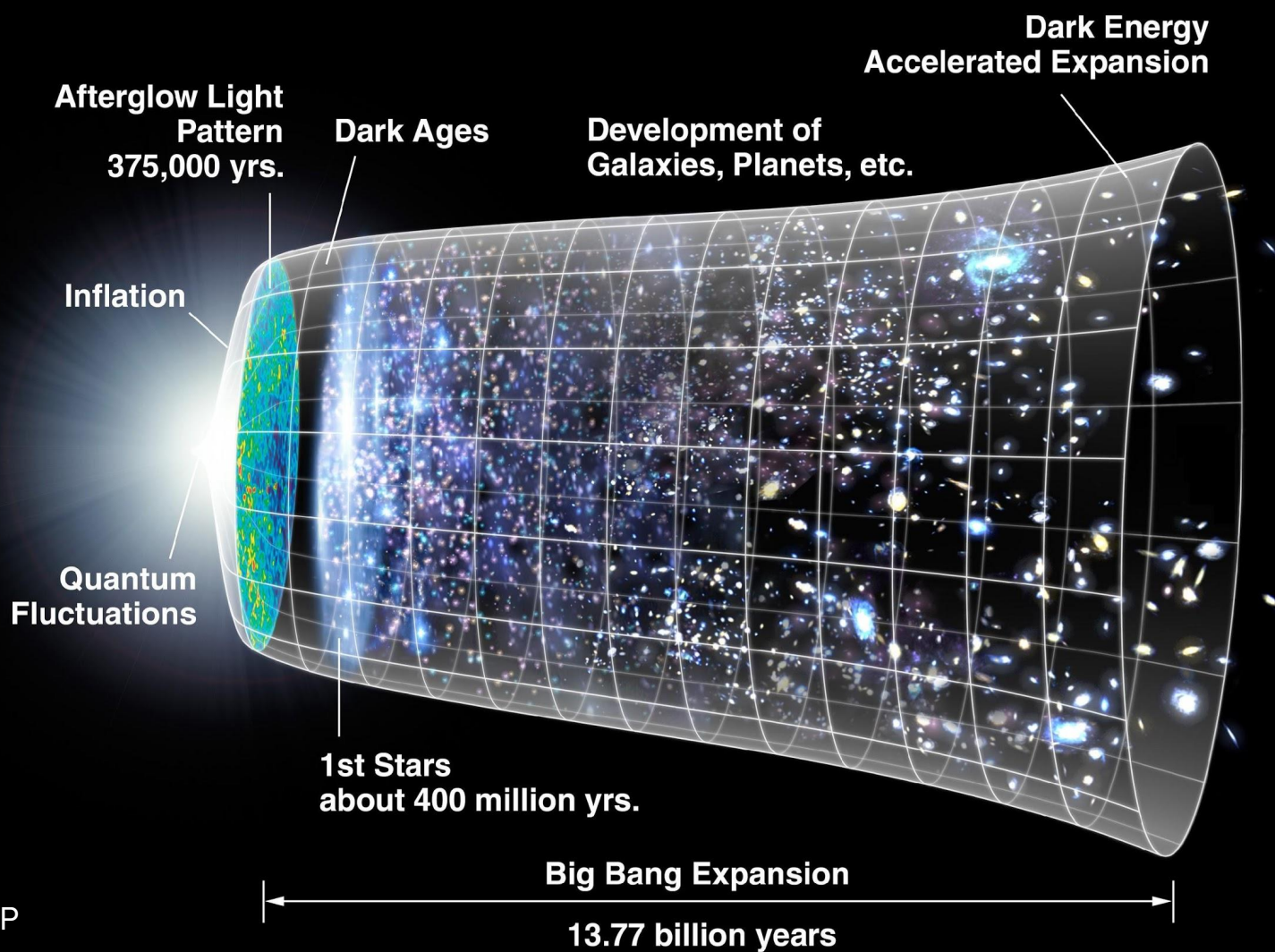
jorlo@sas.upenn.edu

<https://arxiv.org/abs/2105.00068>

Credit: J. Ward



Large Scale Structure and Clusters

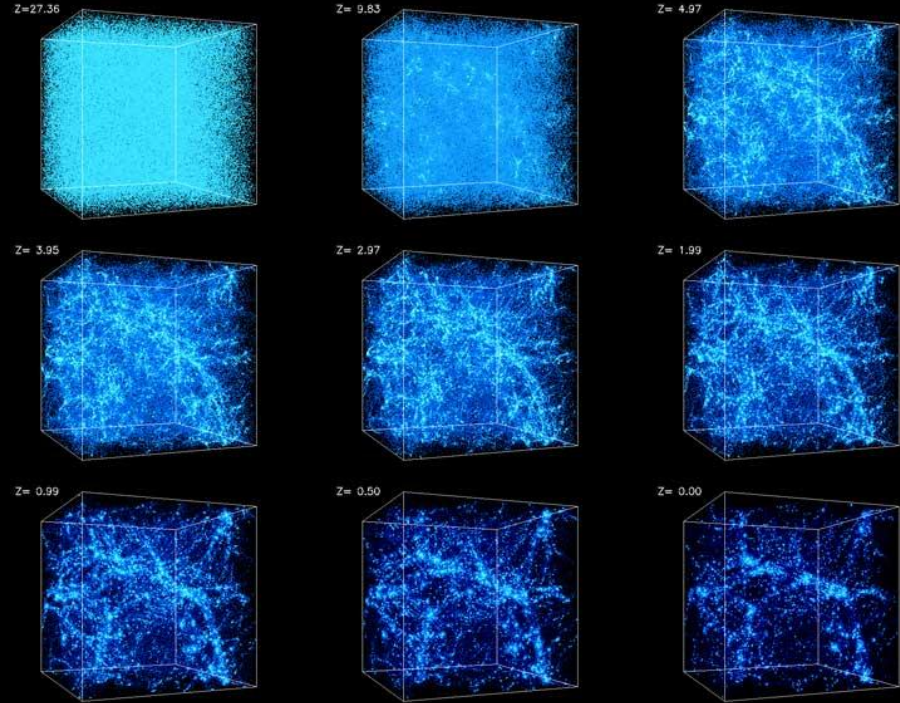


Hierarchical Structure Formation

In Λ CDM model, structure grows
from bottom up

Cluster abundance strong probe
of evolution

Constraints on e.g. neutrino
mass, dark energy equation of
state



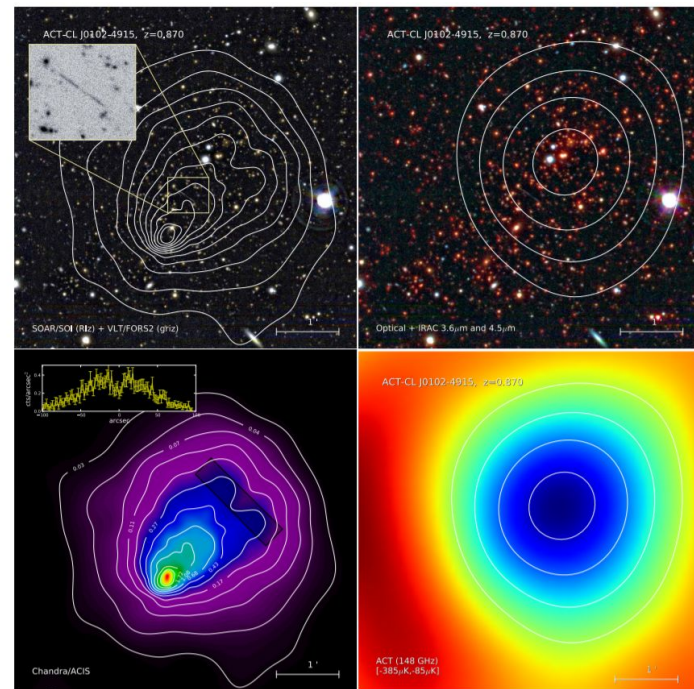
Credit: A. Kravtsov

Cluster Detection

Optical, SZ and X-Ray

What are the selection functions in z and mass?

How do we calibrate mass measurements?



Above: ACT-CL J0102-4915 'El Gordo' in the optical (top left), Optical/IR (top right), x-ray (bottom left) and sub-mm/SZ (bottom right)

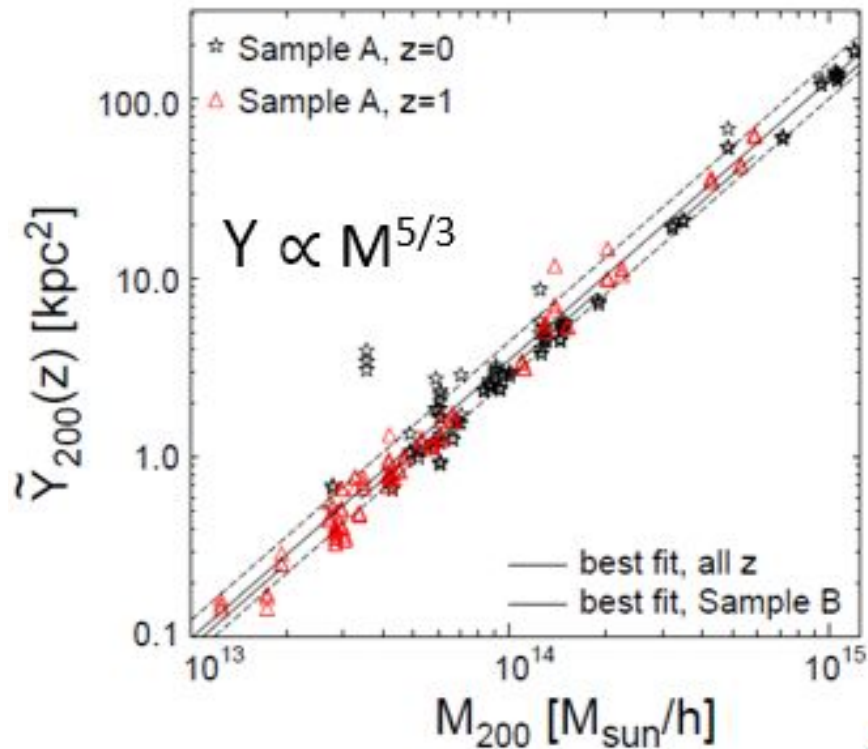
Credit: F. Menanteau, 2012

Abundance Counts and Mass

To do science with the abundance count you need accurate cluster masses

IR/Optical and SZ surveys do not return masses on their own

For SZ surveys, calibrate mass against either X-ray data or weak lensing



Above: Y-M scaling relation calibrated from x-ray data.

Credit: Krause et. al. 2012

Mass/Richness Scaling Relation

SZ and IR/Optical surveys compliment each other

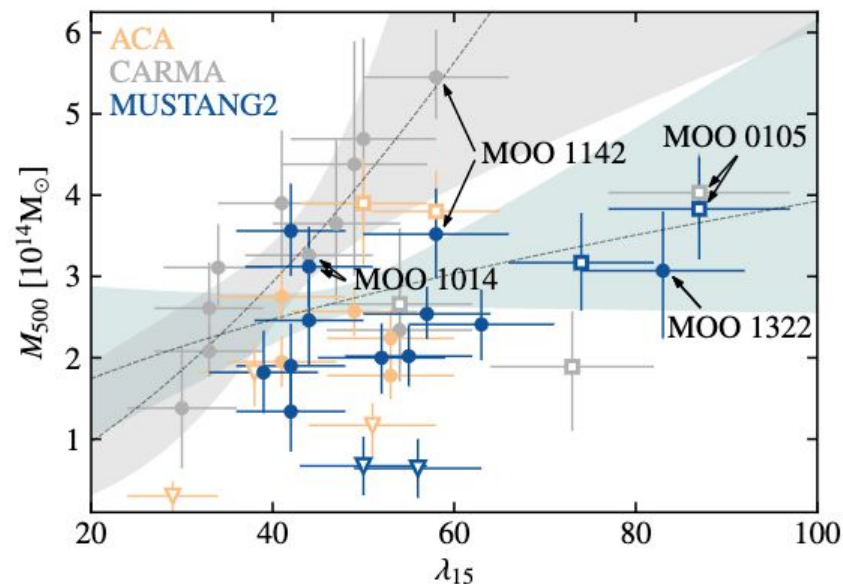
Expect mass of clusters to scale with # of member galaxies

SZ inferred mass allows us to calibrate the mass/richness relation

Of note, the scaling relation is specific to a survey and their definition of richness

Gonzalez 2019 work was preliminary, using a small subset of MaDCoWS clusters

In this work we are extending this fitting to the full MaDCoWS cluster sample using ACT SZ data



Above: Small sample M/λ Grey points and fit are CARMA (Gonzalez et al. 2019). Orange points are VACA LoCA (Di Mascolo et al. 2020). Blue points and fit are MUSTANG2 (Dicker et al. 2020).

Credit: Mroczkowski et al. 2019

MaDCoWS

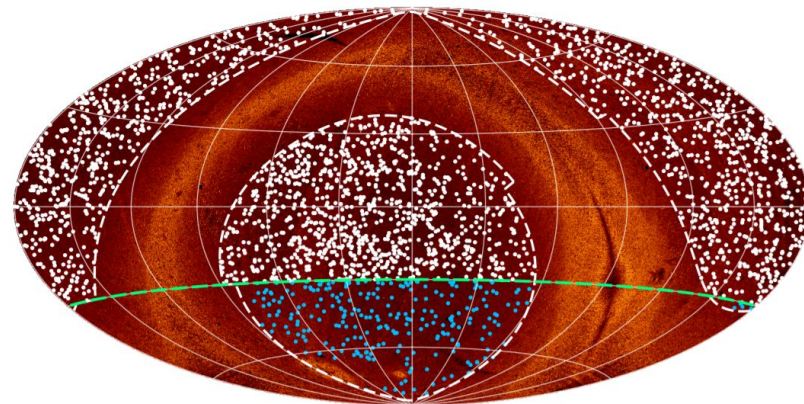
Massive and Distant Clusters of WISE
(MaDCoWS)

IR selected cluster, high z catalog using
WISE data

Color cut to restrict redshift

Limited spectroscopic follow up

Photo z s for most clusters



Above: MaDCoWS survey footprint (dashed lines) over WISE allsky data. Grey dots are clusters with PanSTARRS follow up; blue are clusters with SuperCOSMOS follow up.
Credit: Gonzalez 2019

MaDCoWS Statistics

Galaxy clusters $0.7 \lesssim z \lesssim 1.5$

Photo z 's with $\sigma_z/(1+z) \approx 0.036$ measured using limited spectroscopic follow up

2839 clusters

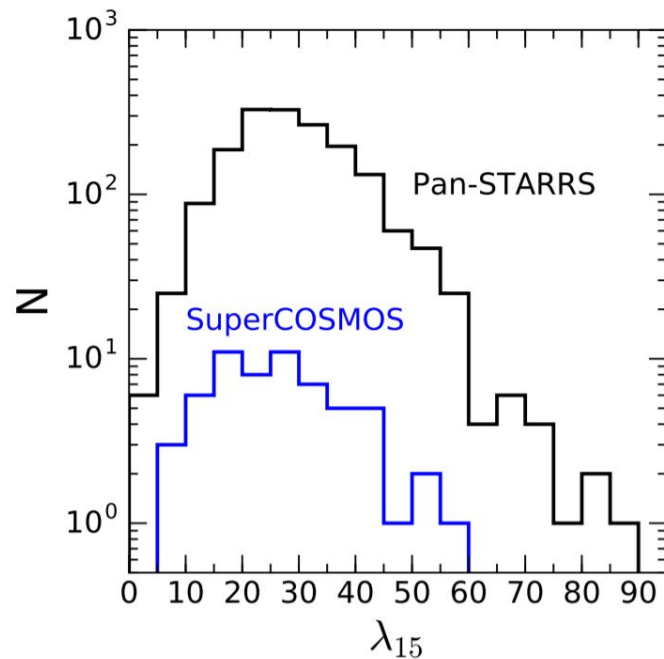
~ 1600 in ACT footprint, 96 codetections

Estimated average mass

$$M_{500} = 1.6 \pm 0.8 \times 10^{14} M_{\odot}$$

For comparison, ACT 90% completeness

$$M_{500c} > 3.8 \times 10^{14} M_{\odot}$$

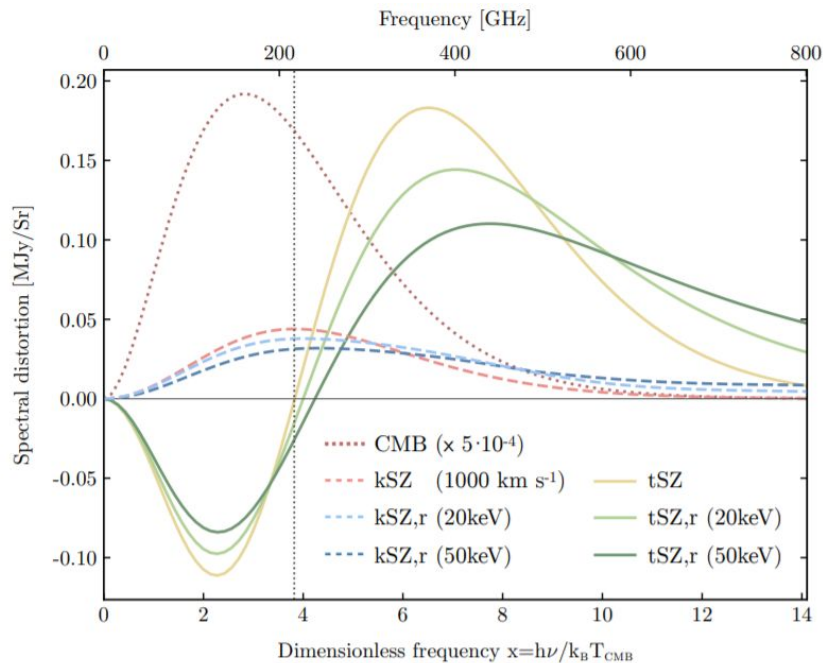


Above: Richness abundance for the MaDCoWS sample.

Credit: Gonzalez 2019

SZ Surveys

Benefits and Drawbacks



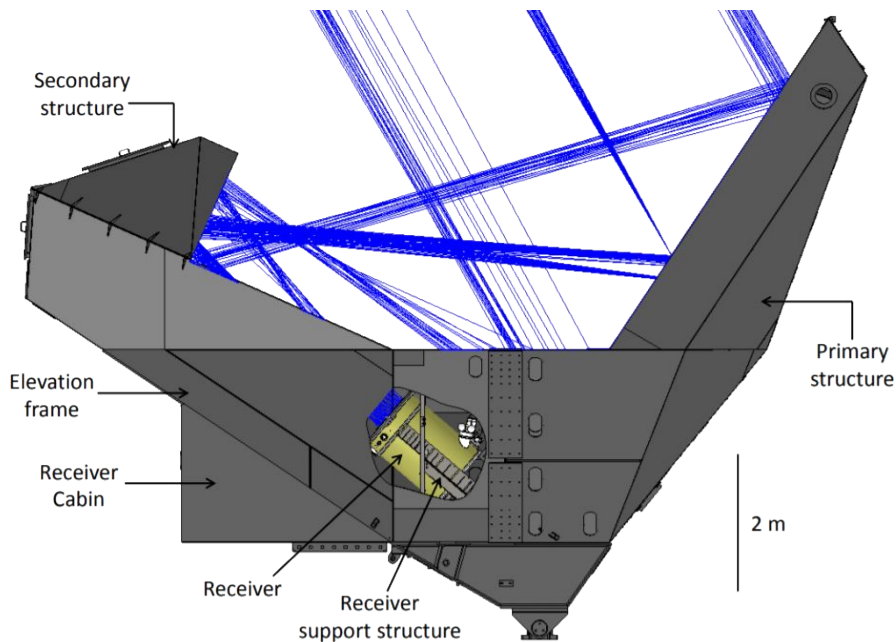
Above: SZ spectral distortion, with CMB spectrum plotted for reference.

Credit: T. Mroczkowski

SZ effect is a spectral distortion: the effect is z independent

Distortion strength scales with mass
Mass calibration required

Low resolution compared to other frequencies (trade-off)



Telescope with receiver.
Credit: R. Thornton

ACT

Atacama Cosmology Telescope

6m off-axis Gregorian

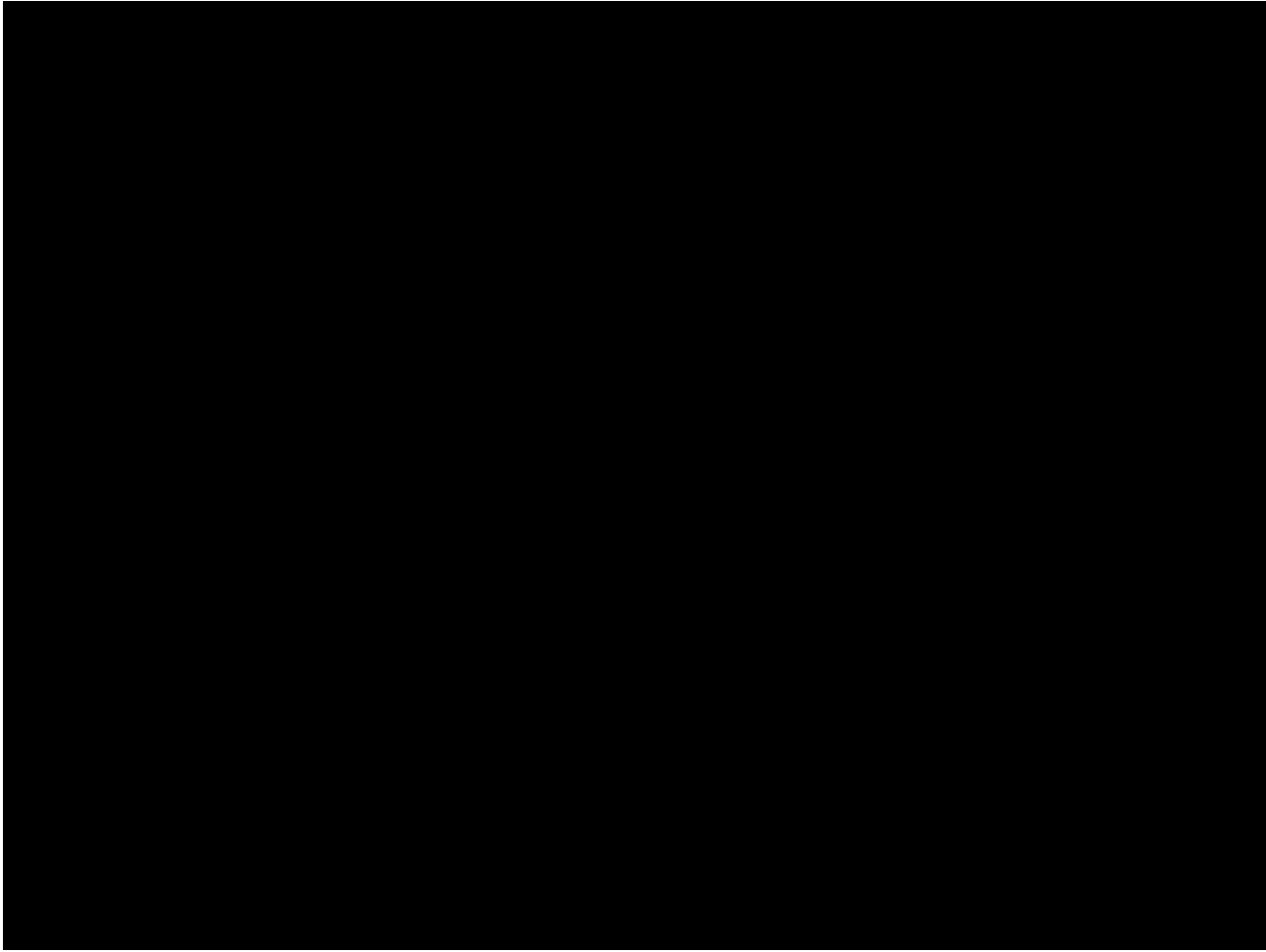
3° FoV

Observations at 90, 150, and
220 GHz

28 and 41 GHz observations
— upcoming

Planck + ACT

Planck



ACT DR5 Cluster Catalog

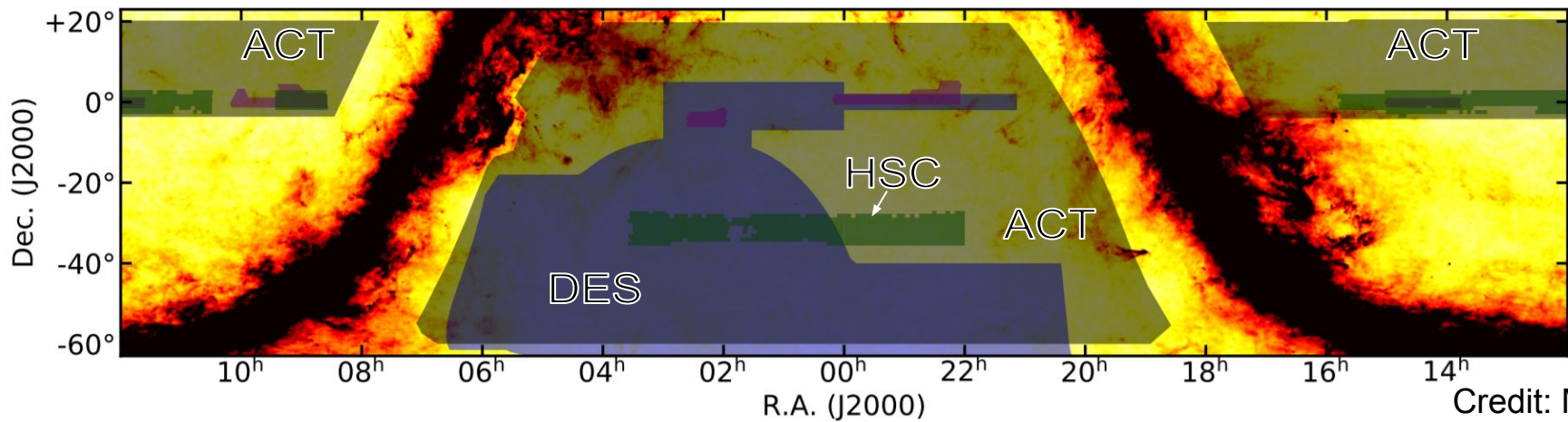
Hilton 2020

4195 SZ selected clusters, optically confirmed

Largest homogeneous sample of SZ-selected clusters to date

Clusters identified over 13,168 square degrees

Significant overlap with optical surveys allows for lensing mass calibration



The ACTxMaDCoWS Mass/Richness Scaling Relation

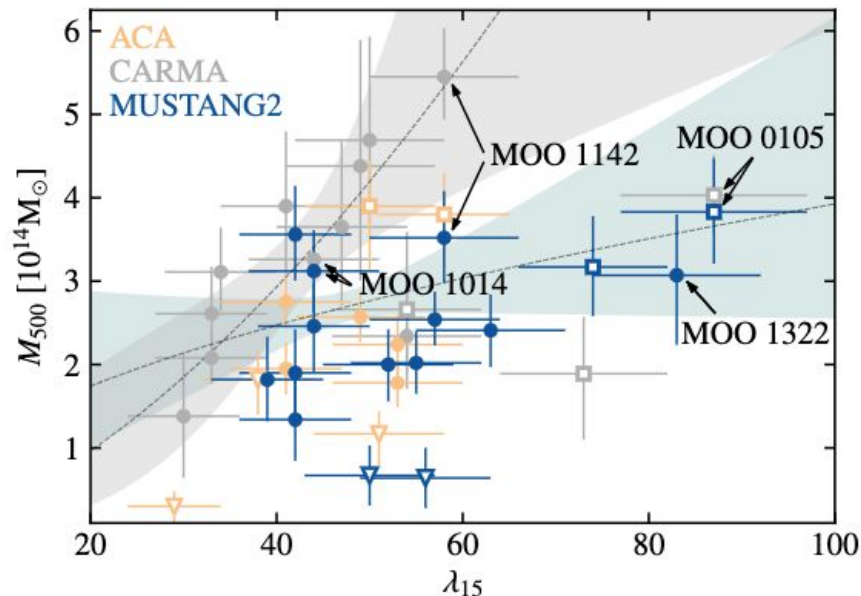
Forced Photometry

Filtered maps of centralized Compton y (\tilde{y}_0)

Map is constructed such that each pixel records the \tilde{y}_0 value that a cluster would have if it was detected at a given location in the map

Simply extract \tilde{y}_0 at locations of MaDCoWS clusters and convert to mass

Resulting masses are free of SZ-selection bias (don't need to be deboosted) but do contain other biases



Above: Richness/SZ relation for MaDCoWS clusters. Black points are binned.

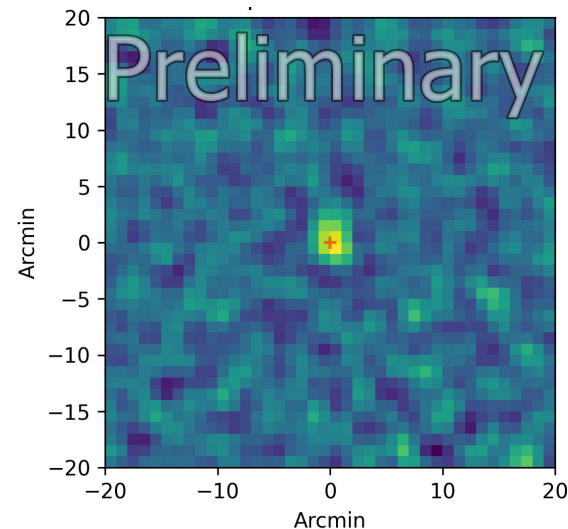
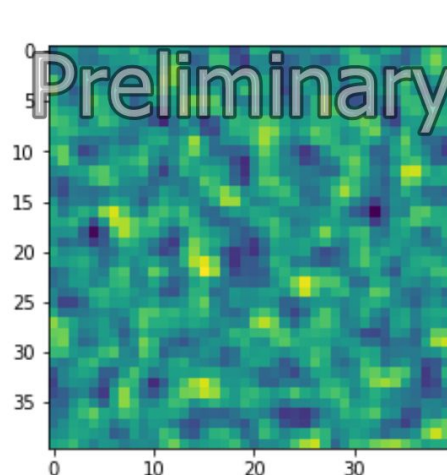
In-Fill of the SZ signal

Matched filter applied to ACT 98 and 150 GHz maps returns \tilde{y}_0 based on a beam convolved filter profile and the shape of the SZ spectral distortion

Emission at 98 and 150 GHz that is spatially correlated with clusters can contaminate \tilde{y}_0 measurement

Preliminary estimates $\sim 1\text{-}2\%$ level on average but a significant component with significant in-fill ($\sim 10\%$ with $\sim 10\%$)

Targeted observations with MUSTANG-2?



Above: ACT (left) and MaDCoWS (right) centered stacks using the ACT 220 GHz map. The SZ distortion at 220 GHz should be zero.

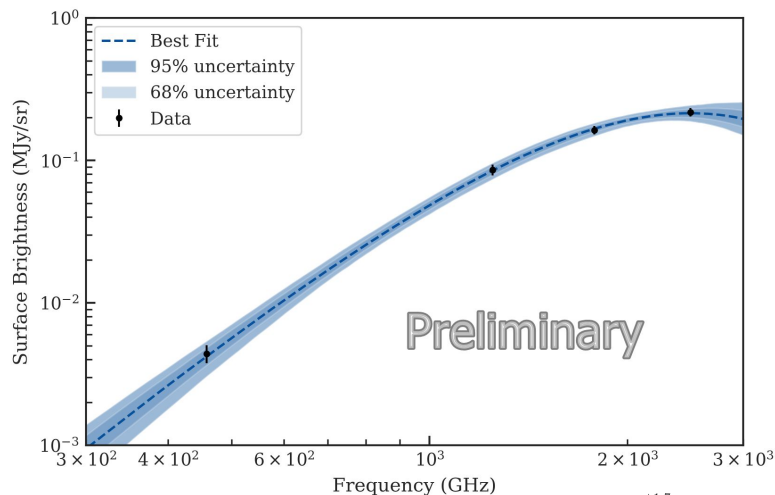
IR Contamination

Evidence for excess IR emission in MaDCoWS clusters as compared to ACT clusters

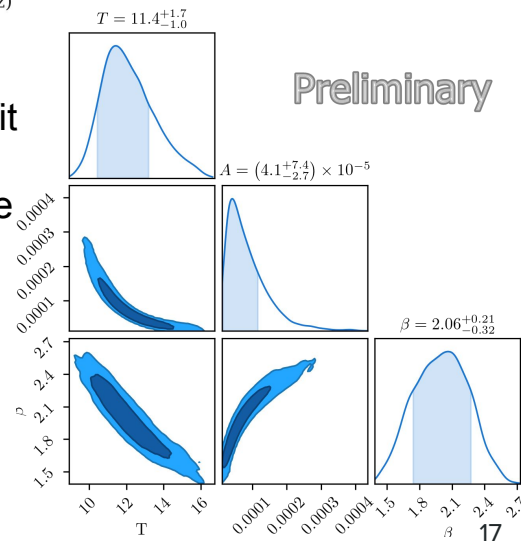
Fit stacks of ACT 220GHz + Herschel 600, 857, and 1200 GHz to a modified grey-body (e.g. attribute flux to dusty emission)

Forced photometry is corrected for this emission

$$\Delta S(\nu) = A(1 - \exp(-(\nu/\nu_0)^\beta)) B_\nu(T_{\text{rest}})$$



Above: Best fit grey-body. Right: Best fit parameters for the above grey-body fit. The fit temperature ($T=11.4^{+1.7}_{-1.0}$ K, rest frame) and spectral index ($\beta=2.06^{+0.21}_{-0.32}$) are both inline with other studies.



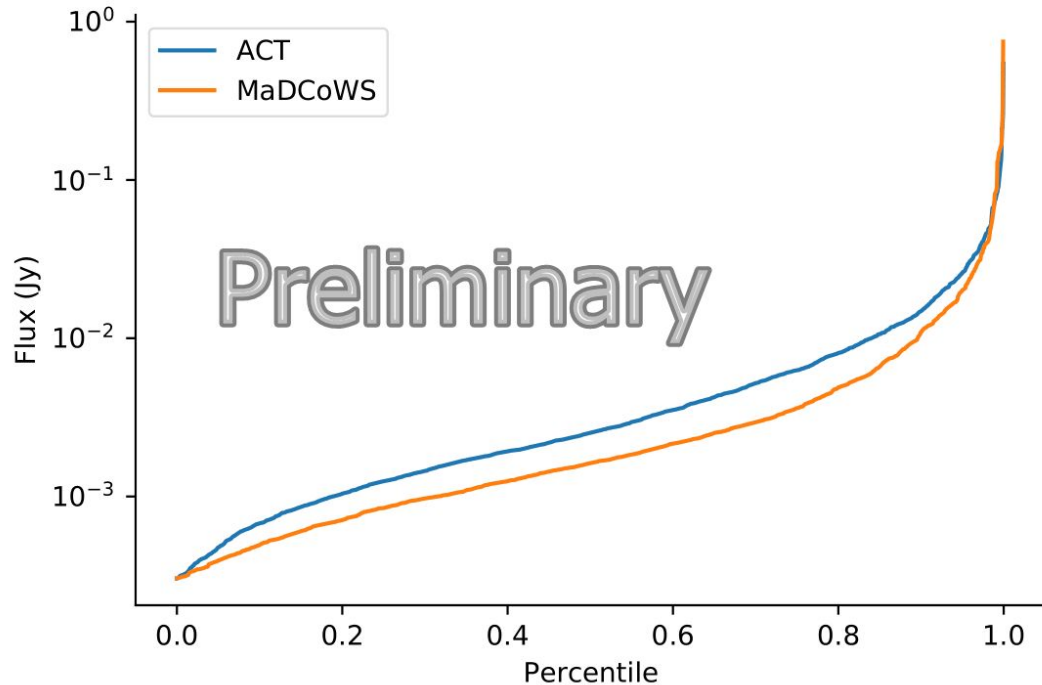
Radio Contamination

ACT clusters show significantly more radio emission than MaDCoWS clusters

Radio fluxes from NVSS (1.4 GHz) and VLASS (3.0 GHz)

Given a simple spectral form of $F(\nu) = C_0 \nu^\alpha$, find a typical spectral index α
 $\alpha = -0.9 \pm 0.7$ for MaDCoWS clusters
and $\alpha = -1.2 \pm 0.8$ for ACT

Similar to IR, remove from forced photometry



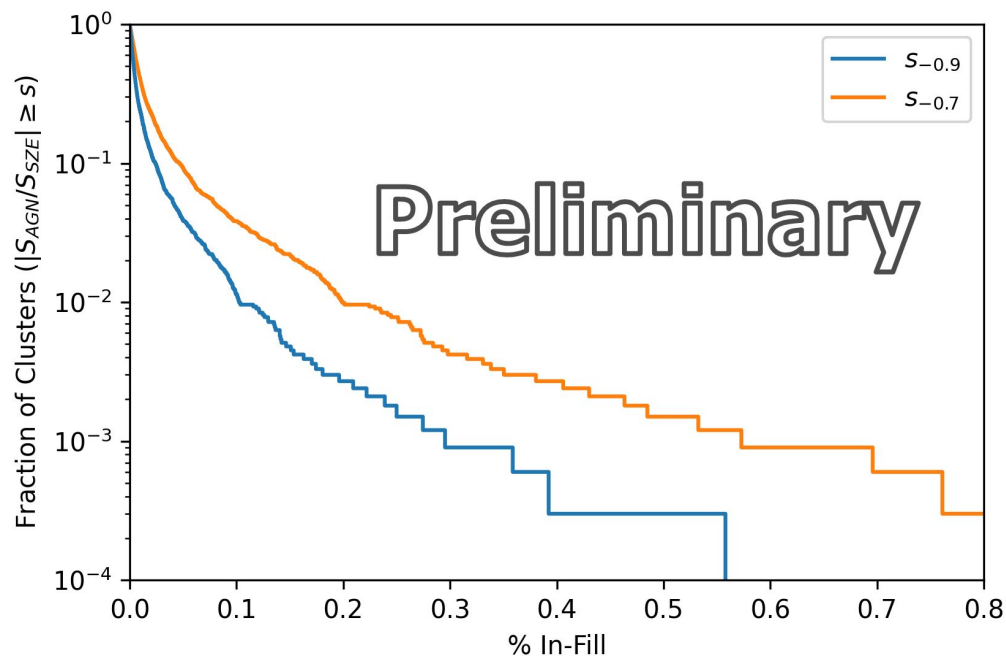
Above: Cumulative histograms for the aperture flux at 1.4 GHz for ACT and MaDCoWS clusters above 1σ noise. The two distributions are different at very high significance ($\sim 17\sigma$). The ACT median flux for the full sample is 6.1 ± 0.4 mJy, and the MaDCoWS is 3.9 ± 0.4 mJy. Fluxes preliminary

In-Fill Results

Extrapolate radio flux from NVSS (1.4GHz) to 98 and 150GHz

Average contamination is low (1-2%) but significant fraction with significant contamination (10% with 10%)

Extremely sensitive to spectral index: measurements needed near observation frequencies (98 and 150)



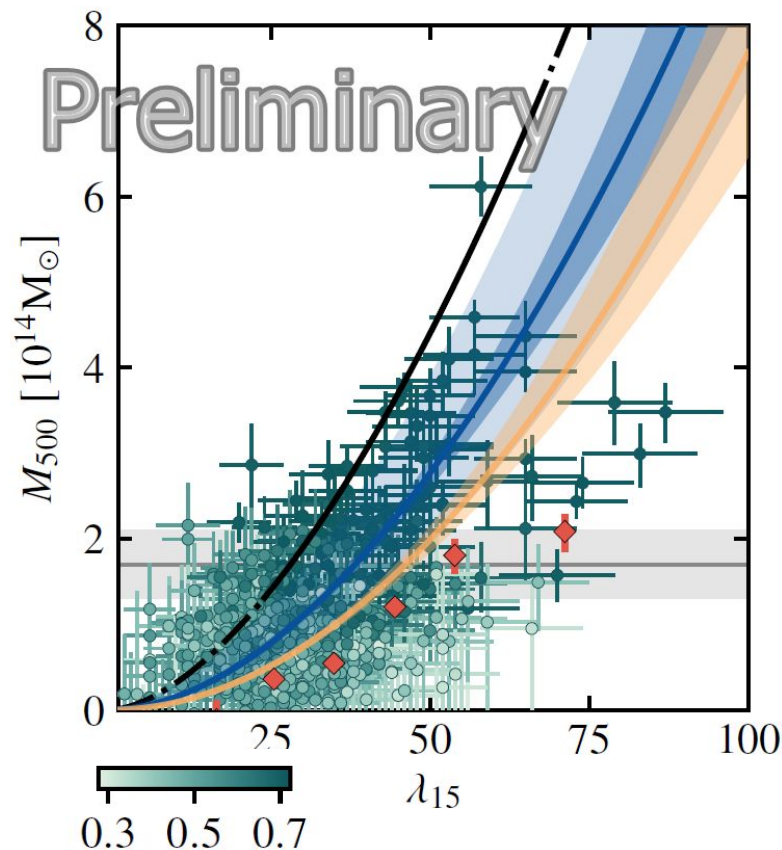
Above: ACT cluster in-fill extrapolated from 1.4GHz assuming $\alpha = -0.9$ (blue) and $\alpha = -0.7$ (orange)

Mass/Richness Scaling

Fit to a mixture model which included a population which is a normal distribution about power-law $M \propto (\lambda_{15})^\kappa$ for κ the slope and a noise-like population normally distributed about 0

Each data point has a fit weight, which is the probability of belonging to the mass-richness power-law

Power-law slope κ is a fit variable with best fit $\kappa = 1.84 \pm 0.15$



Best fit mass-richness scaling relation with (blue) and with out (orange) noise-like population

$$f_v(\xi, \eta, \theta_{\text{radio}}, \theta_{\text{dust}}) = c(\xi) \cdot m_v(\eta) + g_v [d_v(\theta_{\text{dust}}) + r_v(\theta_{\text{radio}})] \quad 20$$

Simons Observatory and the Future

The Simons Observatory

Next generation CMB observatory

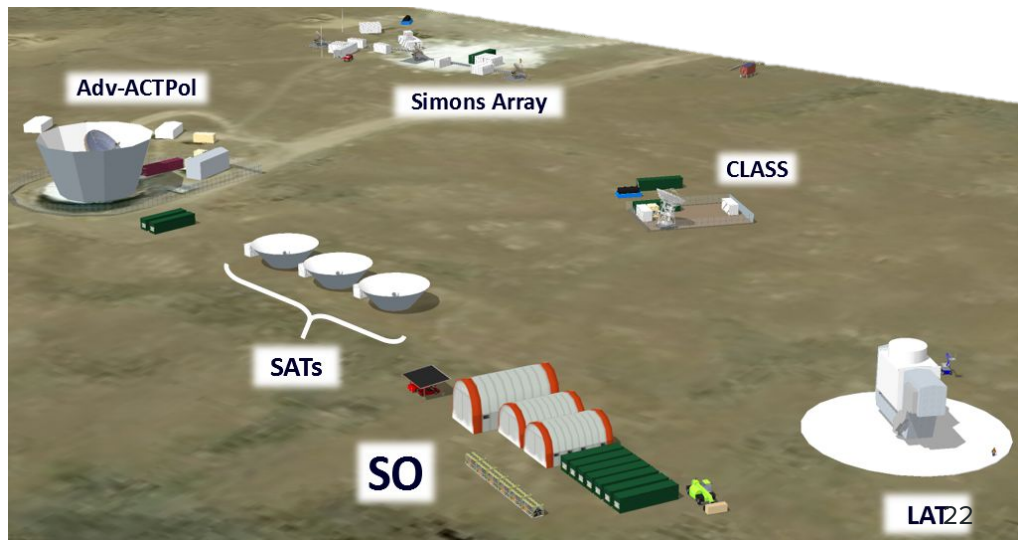
One large aperture telescope (LAT) and 3 small aperture telescopes (SATs)

Order of magnitude increase in detector count

~40K in the LATR and ~30K across the SATs, with capability to expand to >80K in LATR

LAT primarily concerned with small angular scale science

SAT covers large angular scales



Clusters with SO

Factor ~5 increase in cluster counts

At least 16k clusters, hoping for 24k
at $S/N > 5$

Clusters out to $z \sim 3$

Fractional mass calibration $> 10\%$

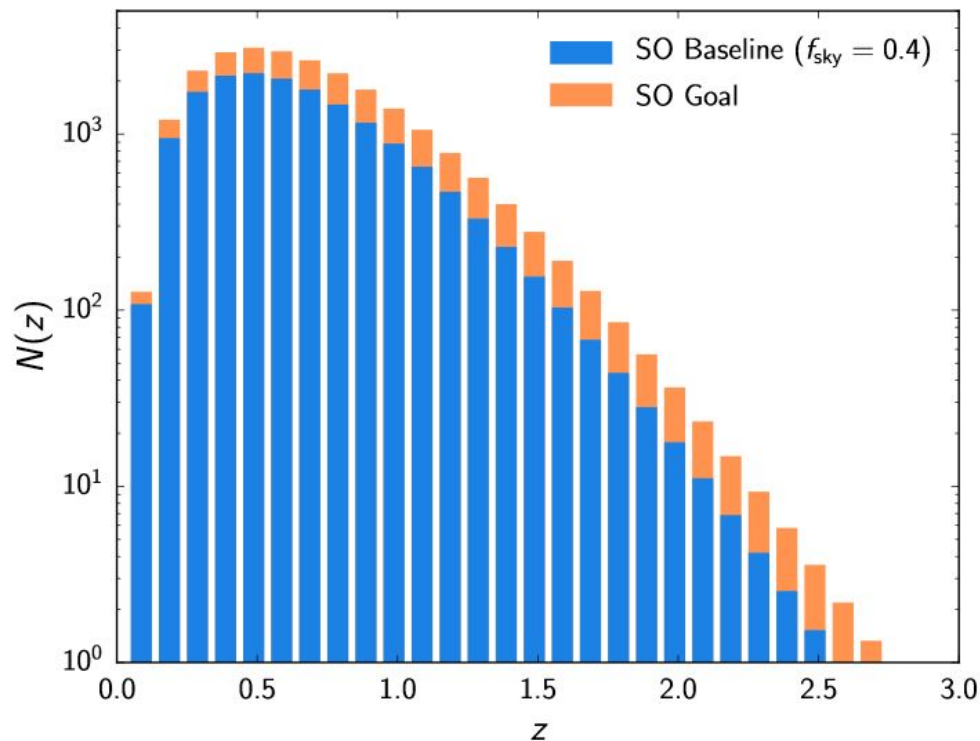
For $z > 1$, $1.5 \times 10^{14} M_{\odot} < M < 2.5$

Sky coverage $\sim 40\%$

Excellent overlap with up coming optical and
IR surveys

See SO Science paper for details:

<https://arxiv.org/abs/1808.07445>



Above: Cluster abundance as a function of z for SO Baseline (blue) and Goal (orange)

Conclusions

Conclusions

The cluster abundance function is a strong probe of cosmology at large scales

A careful accounting of all clusters and accurate estimations of their masses necessary for precision cosmology

Understanding SZ in-fill is necessary for precise abundance function and requires high resolution measurements of point source flux densities as well as measurements of spectral indices near frequencies of interest

Future is bright with next generation experiments promising factor of several increase in cluster catalogs

Backup slides

Optical/IR Surveys

Based on spatial galaxy overdensities

No intrinsic measure of cluster mass, only # of associated galaxies (richness, or λ)

Specifics of richness definition vary from survey to survey

In addition to spatial correlation, galaxies in cluster should be correlated in redshift

Spectroscopic follow up is limited, generally use a color cut

Line of sight coincidences i.e. interlopers



Above: Artist conception of Wide-field Infrared Survey Explorer (WISE)

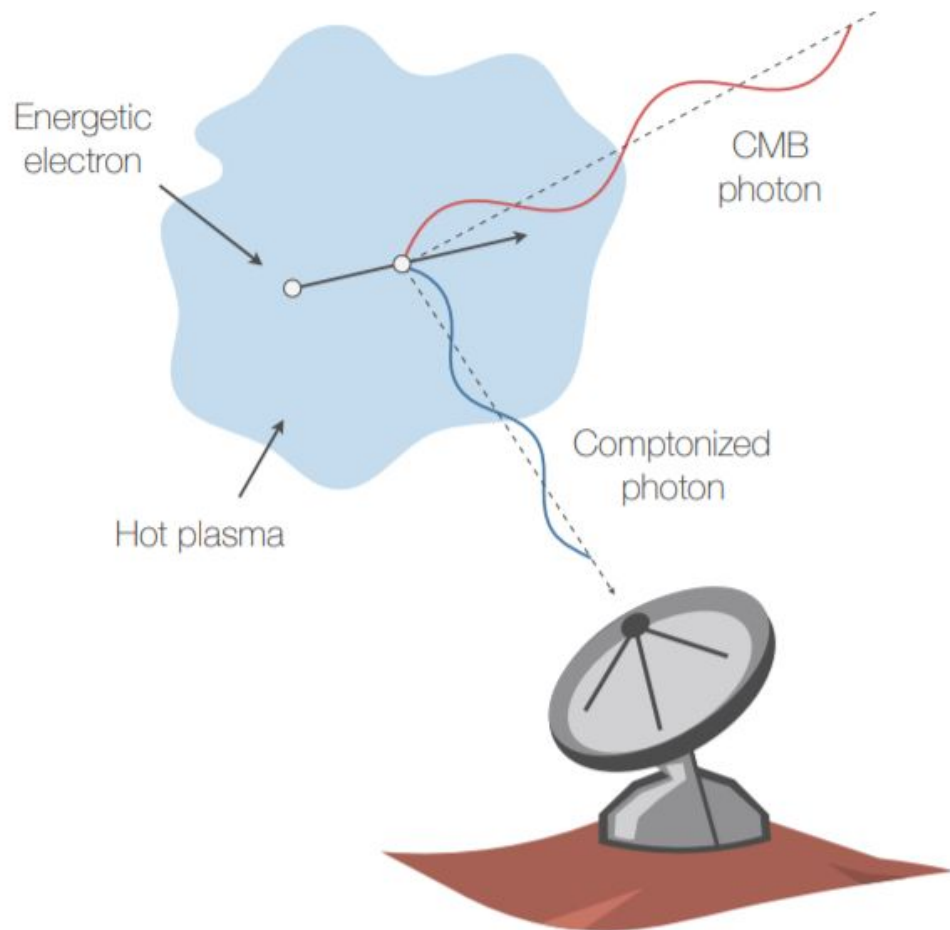
Credit: NASA/JPL-Caltech

sub-MM/CMB Surveys and the SZ Effect

Identify clusters via SZ effect

Inverse Compton scattering leads to
blue-shifting of CMB photons

CMB ‘backlights’ the clusters



ACT DR5

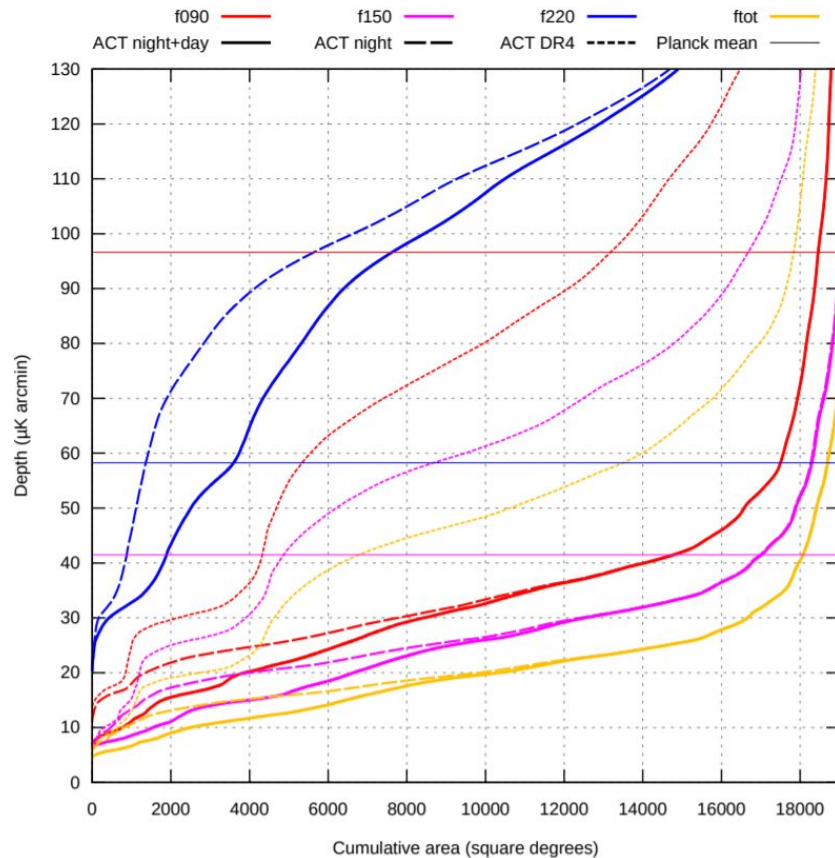
Data released through 2018

Significant resolution improvement over Planck

Now deeper than Planck over much of the sky at 90 and 150 as well

Approximately 18,000 square degrees of sky coverage

Data in the can through 2020 and observations continuing at least through 2021



Above: ACT map depth at 90, 150, and 220 GHz for the latest data release (solid) and various splits. Horizontal lines show average Planck map depths.

Credit: S. Naess 2020

ACT Catalog Statistics

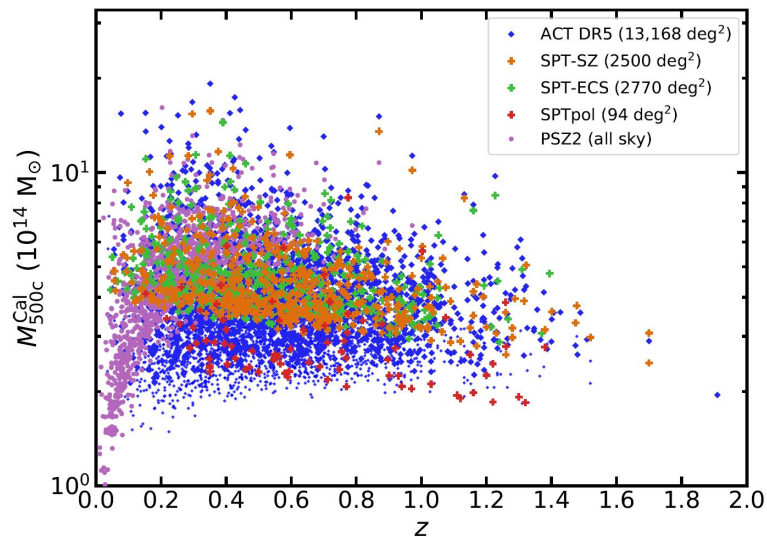
$0.04 < z \leq 1.91$, $z_{\text{median}} = 0.52$, 221 w/ $z > 1$,
436 w/ $z > 0.9$

90% completeness $M_{500c} > 3.8 \times 10^{14} M_{\odot}$ at
 z_{median}

~1600 MaDCoWS clusters in ACT footprint, 96
Codetections (at ≥ 4 -sigma)

Expect catalog to add an additional 3-5,000
clusters with the final ACT data releases

Code is publicly available [here](#) and the catalog
itself is publicly available [here](#)



Above: ACT DR5 cluster catalog
compared to other blind SZ surveys

Credit: M. Hilton

Deviations from Self-Similarity

Interlopers may bias richness high,
increasing slope

Similarly, a significant portion of low
richness clusters may be chance
coincidences

No richness dependence in IR
correction due to a lack of data

The high radio contamination clusters
do not bias slope significantly

Above: Variation of fit with S/N cuts. Removing low
S/N clusters restores reasonable slopes.

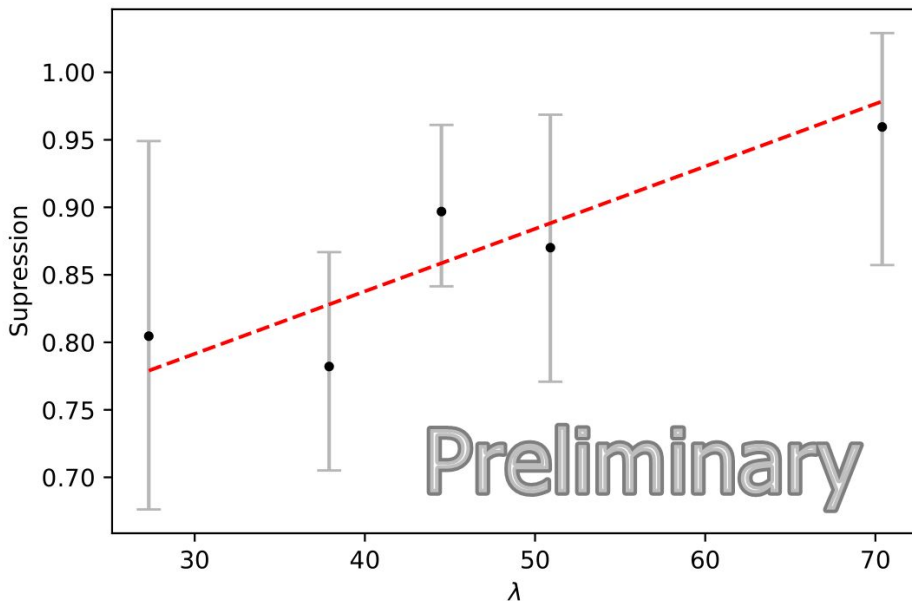
Centroid Offset

MaDCoWS reported position is peak of a smoothed galaxy density map

The cluster location identified can be offset from the center of the cluster mass, and hence SZ signal

By comparing amplitude of stacks on ACT center and MaDCoWS center, can quantify effect

Slight richness dependence



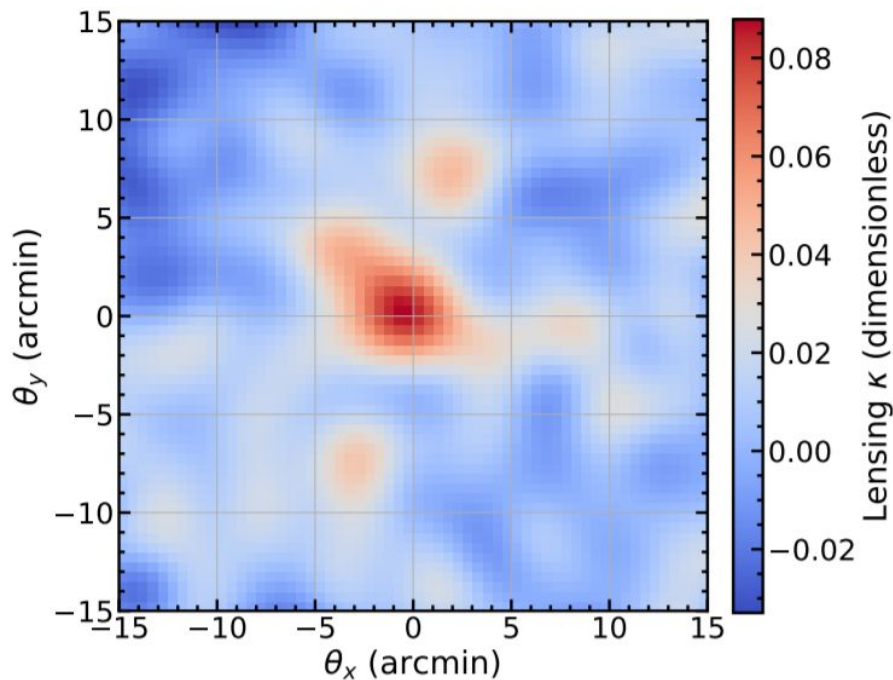
Above: SZ signal suppression as a function of richness for ACT/MaDCoWS co-detections.

Lensing Mass

M. Madhavacheril 2020 recovered averaged mass of MaDCoWS subsample (using lensing of the CMB

4.2 σ detection

Average mass $M_{500} = 1.7 \pm 0.4 \times 10^{14} M_{\odot}$, consistent with both the mass from the Gonzalez 2019 preliminary fit and our averaged forced photometry mass, $1.3 \pm 0.7 \times 10^{14} M_{\odot}$ for all clusters with richness and $1.7 \pm 0.8 \times 10^{14} M_{\odot}$ for 1σ clusters

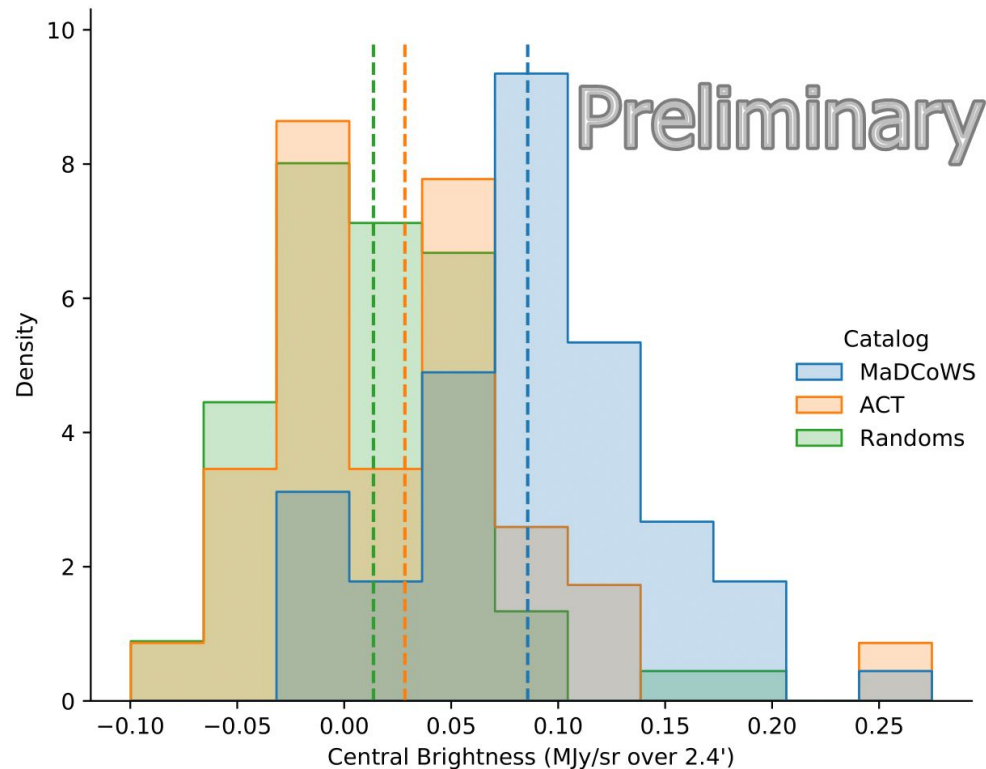


Population Difference

IR and radio data point to ACT and MaDCoWS drawing from different underlying cluster populations

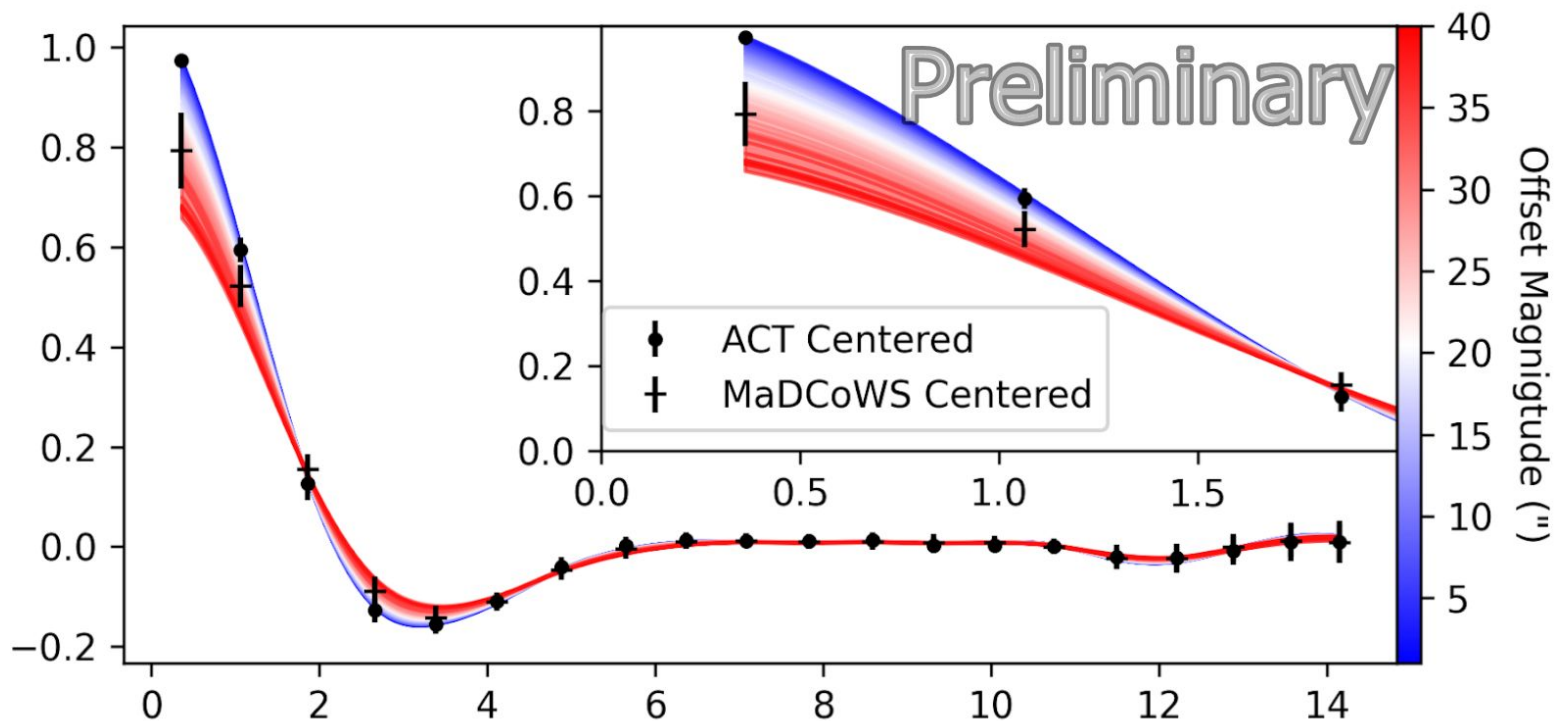
One, dustier population is preferentially sampled by the MaDCoWS survey, and the other, more virialized and radio bright, is preferentially sampled by ACT

Survey biases are not unexpected

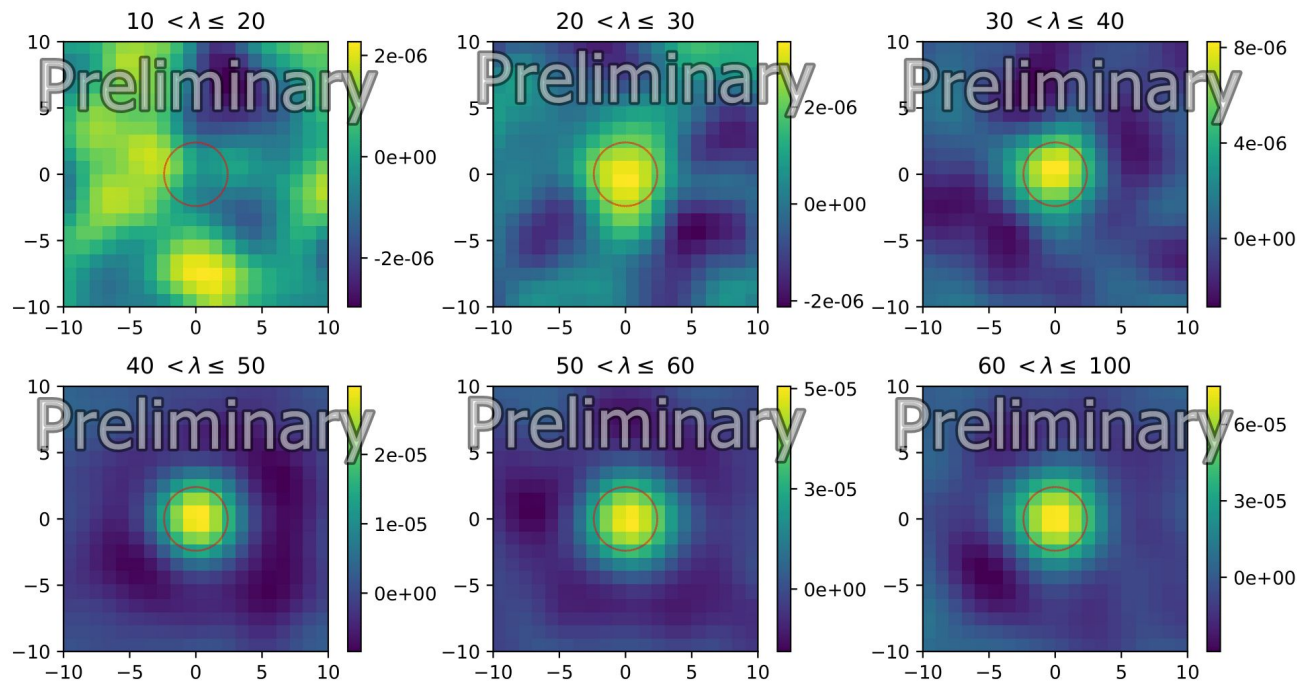


Above: Histogram of MaDCoWS and ACT cluster 500 μ m surface brightness. A sample of random points is shown for comparison.

Centroid Offset



Stacked Results



Stacked SZ on MaDCoWS cluster locations in richness bins. Excess is statistically significant in all bins except 10-20

Matched Filter

See Hilton 2020 Sec. 2.2 and 2.3

$$\psi(k_x, k_y, \nu_i) = A \sum_j \mathbf{N}_{ij}^{-1}(k_x, k_y) f_{\text{SZ}}(\nu_j) S(k_x, k_y, \nu_j).$$

For A a normalization, N the noise covariance, f_{SZ} is the non-relativistic form of the SZ spectral dependence, S is a beam-convolved signal template, where the signal template is an Arnould 2010 UPP with $M_{500} = 2 \times 10^{14} M_{\odot}$ at $z = 0.4$

Convert to mass:

$$\tilde{y}_0 = 10^{A_0} E(z)^2 \left(\frac{M_{500c}}{M_{\text{pivot}}} \right)^{1+B_0} Q(\theta_{500c}) f_{\text{rel}}(M_{500c}, z),$$

Where A_0 is a normalization, E is the redshift evolution of the hubble parameter, B and M_{pivot} are parameters of the UPP, f_{rel} is the relativistic correction, and Q is a mismatch function that quantifies the difference in angular size b/w the reference filter scale and the specific cluster scale given M and z